

# An NMF-Based Methodology for Selecting Biomarkers in the Landscape of Genes of Heterogeneous Cancer-Associated Fibroblast Populations

Bioinformatics and Biology Insights  
Volume 14: 1–13  
© The Author(s) 2020  
Article reuse guidelines:  
sagepub.com/journals-permissions  
DOI: 10.1177/1177932220906827



Flavia Esposito<sup>1\*</sup>, Angelina Boccarelli<sup>2</sup> and Nicoletta Del Buono<sup>3\*</sup>

<sup>1</sup>Department of Electronic and Information Engineering, Politecnico di Bari, Bari, Italy.

<sup>2</sup>Department of Biomedical Science and Human Oncology, University of Bari Medical School,

Bari, Italy. <sup>3</sup>Department of Mathematics, University of Bari Aldo Moro, Bari, Italy.

**ABSTRACT:** The rapid development of high-performance technologies has greatly promoted studies of molecular oncology producing large amounts of data. Even if these data are publicly available, they need to be processed and studied to extract information useful to better understand mechanisms of pathogenesis of complex diseases, such as tumors. In this article, we illustrated a procedure for mining biologically meaningful biomarkers from microarray datasets of different tumor histotypes. The proposed methodology allows to automatically identify a subset of potentially informative genes from microarray data matrices, which differs either in the number of rows (genes) and of columns (patients). The methodology integrates nonnegative matrix factorization method, a functional enrichment analysis web tool with a properly designed gene extraction procedure to allow the analysis of omics input data with different row size. The proposed methodology has been used to mine microarray of solid tumors of different embryonic origin to verify the presence of common genes characterizing the heterogeneity of cancer-associated fibroblasts. These automatically extracted biomarkers could be used to suggest appropriate therapies to inactivate the state of active fibroblasts, thus avoiding their action on tumor progression.

**KEYWORDS:** NMF, metagene, microarray, cancer, fibroblast, cancer-associated fibroblast

**RECEIVED:** October 13, 2019. **ACCEPTED:** January 22, 2020.

**TYPE:** Original Research

**FUNDING:** The author(s) disclosed receipt of the following financial support for the research, authorship, and/or publication of this article: This work was supported in part by the GNCS-INDAM (Gruppo Nazionale per il Calcolo Scientifico of Istituto Nazionale di Alta Matematica) Francesco Severi, P.le Aldo Moro, Roma, Italy.

**DECLARATION OF CONFLICTING INTERESTS:** The author(s) declared no potential conflicts of interest with respect to the research, authorship, and/or publication of this article.

**CORRESPONDING AUTHOR:** Flavia Esposito, Department of Electronic and Information Engineering, Politecnico di Bari, via E. Orabona 4, I-70125 BARI, Italy.  
Email: flavia.esposito@poliba.it

## Introduction

Complex human diseases are caused by the interactions of many genetic, environmental, and behavioral factors. Development of high-performance technologies greatly promoted studies on molecular oncology producing large amounts of omic data. The availability of massive volume of experimental data based on cancer researches requires the development of mathematical, statistical, and computational techniques, which automatically extract valuable information useful for a better understanding of pathogenesis mechanisms of complex diseases, such as tumors. Identifying marker genes potentially involved into the development of tumors may facilitate the understanding of cause of disease, thus contributing to the advancement of diagnostic tools and/or to the evaluation of more efficient clinical strategies.

In most of the publicly available data sets, the number of genes is significantly larger than the number of samples. This high dimensionality represents a major problem for an automatic gene array-based cancer analysis. In this scenario, dimensionality reduction methods became indispensable as they can eliminate irrelevant and redundant information, thus reducing the dimensionality as well as the complexity of the original problem, with significant benefits in terms of computational efficiency, model interpretability, and data understanding.

Among linear dimensionality reduction methods, low rank matrix decomposition algorithms have been successfully

exploited as alternative approaches for studying various types of high-dimensional biological data, including gene expression data.<sup>1</sup> The application of these algorithms relies on the assumption that large-scale biological data have an intrinsic low-dimensional representation, with the dimension often corresponding to the number of latent information embedded into the original data. These methods transform the space of original data into a lower dimensional more discriminating (informative) space that makes the subsequent analysis more efficient.

Among low-rank reduction mechanisms, nonnegative matrix factorizations (NMFs) emerge as useful approaches for the analysis of microarray data. The intrinsic non-negativity property of these techniques, in fact, produces more intuitive results as many biological measurements are represented by positive values. Nonnegative matrix factorizations demonstrated their ability in a number of tasks, including the identification of sets of genes co-operating in a relatively tightly regulated manner;<sup>2</sup> the discovery of potential relationships in large biological data samples and link genes to these patterns;<sup>3</sup> the detection of distinct genomic subtypes in cancer patients;<sup>4</sup> the inspection of expression data sets including time evolution of the gene expression profile in different samples;<sup>5</sup> and the extraction of gene expression profiles from fibroblasts of cancer blood diseases.<sup>6</sup>

In this article, we present a gene extraction methodology, which integrates a NMF method<sup>7,8</sup> with the functional enrichment analysis web tool WebGestalt<sup>9</sup> and a gene extraction

\* INDAM Research Group GNCS.



procedure designed ad hoc to automatically mine different microarray cancer data sets to extract a reduced subset of genes to be further investigated from a biological point of view. An approach for mining multi-omics cell line data with the same row size by joint nonnegative matrix factorization (JNMF) and pathway signature analyses was recently proposed in Fujita et al.<sup>10</sup> The methodology presented in this article instead allows to analyze microarray data matrices, which differ either in the number of rows (genes) and in the number of columns (patients) to verify the presence of common genes characterizing the heterogeneity of different cancer datasets. This proposal enriches the panorama of large-scale data-driven computational methods based on matrix factorization algorithms, which are able to extract concise and useful pieces of information from existing disease-associated data sets.<sup>1,11,12</sup> Particularly, through the NMF method, our methodology mines the metagenes, which are the most representative of the information embedded into different tumor datasets and then, by simple intersection set operations allow to extract genes in a natural way to obtain interpretable and useful knowledge readily usable from biologists and analyzed, thanks to functional and visualization approaches based on the WebGestalt tool. The proposed methodology has been used to mine microarray of solid tumors of different embryonic origin to verify the presence of biomarkers characterizing the heterogeneity of cancer-associated fibroblasts (CAF) thus being applicable in clinical practice.

Fibroblasts constitute the most heterogeneous and abundant population of mesenchymal cells in tumor microenvironment (TME). Their presence goes from tumor formation up to the final stage of metastatic diffusion, but their precise functional role in tumor is not fully understood yet.<sup>13</sup> Also, it is not clear how different subtypes of CAF could exert distinct paracrine actions affecting specific tumor oncogenesis.<sup>14,15</sup> Therefore, we adopt the proposed procedure to analyze gene expression profiles of CAFs belonging to primary cultures of 3 distinct tumor histotypes (ie, colon of endodermal origin, breast carcinoma of ectodermal origin and ovary of mesodermal origin) to select common biomarkers and characterize activated fibroblast phenotype. Moreover, as it is known that bone marrow (BM) is a CAF recruitment source,<sup>16</sup> we aim at investigating also the existence of common genes among CAF gene expression profiles of selected solid tumors and those of BM of patients with multiple myeloma (MM) and monoclonal gammopathy of undetermined significance (MGUS; MGUS is a benign pathological condition characterized by the proliferation of a plasma cell clone that rarely evolves into a malignant neoplasm.<sup>17</sup> The latter, being a benign pathological condition, simulates a well-differentiated CAF phenotype compared to those of patients with MM.). Using the proposed methodology, we highlight the existence of biomarkers among CAFs of different embryonic origin that uniquely identify them and could be useful for developing or evaluating more efficient clinical strategies.

This article is organized as follows. First, the pipeline of the whole gene extraction methodology is presented, illustrating a

general way to pre-process this kind of data, its analysis core (based on the NMF method), and the ad hoc gene landscape extraction procedure. The subsequent section describes the specific biological problem we investigated, as well as the databases of CAF populations used in the experimental session. Then, the functional and pathway analysis performed during the experiments are deeply discussed and the obtained results are highlighted from a biological point of view. Some conclusive remarks conclude the article.

## Methods

This section discusses in some detail the main architecture, data pre-processing, and basic NMF approach used in this study.

### *The ensemble gene extraction methodology*

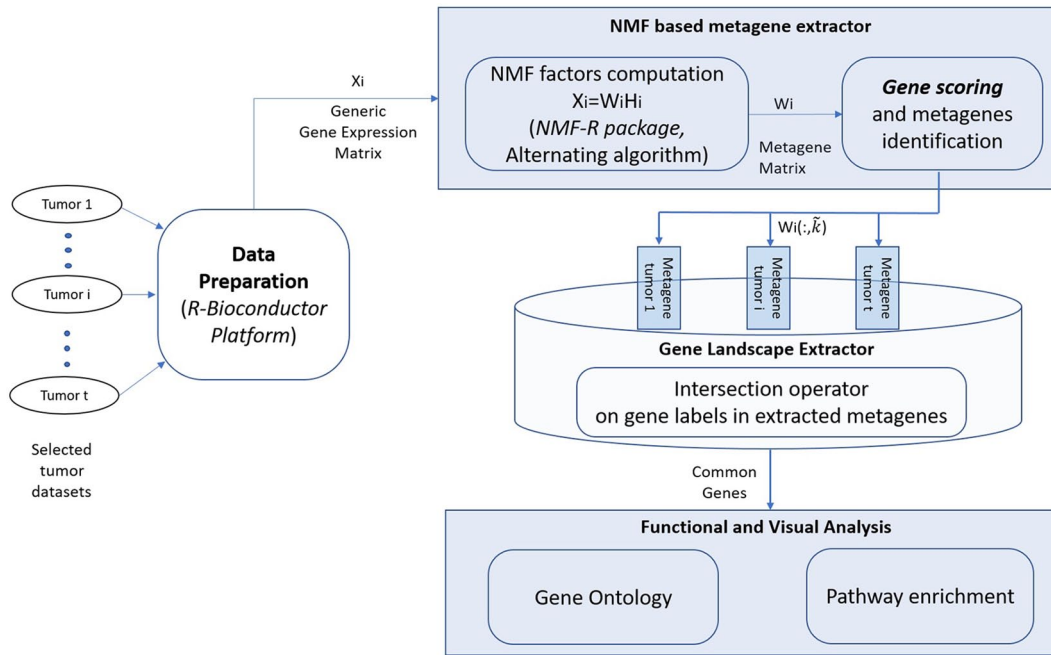
The proposed methodology is based on different operations that integrate the acquisition of data, their mathematical analysis, and the biological exploration of the obtained results.

Figure 1 illustrates the work-flow and the main operations performed when selected tumor data sets are provided.

The methodology is mainly based on the integration of 4 parts: the data preparation module, the core module computing NMF of given data matrices, the Gene Landscape extractor devoted to the extraction of common genes between processed results, and the Functional and Visual Analysis module. The first 3 modules combine R/BioConductor platform and the NMF library, which are well established in bioinformatics research,<sup>18–20</sup> whereas the biological analysis of the latter module is performed using the well-known web tool WebGestalt.

*Data preparation and pre-processing.* Working on microarray data requires data sets are imported in the virtual environment as a single different expression set, in which probeset represents gene interrogating a  $X \in \mathbb{R}_+^{n \times m}$  particular expressed sequence.<sup>21</sup> Once the data set is loaded, a pre-processing phase needed to be applied to create a correspondence between probeset and gene symbol. Data preparation module allows to handle gene expression set in which probesets map the same gene even when they refer to different quantities of transcript or to tackle the associated probes, which were not annotated in any sequence. Figure 2 explains the cases treated by this phase to create gene expression data feeding the following algorithms.

The pre-processing operations implemented in this module are based on the adjusted median absolute deviation (MAD) of the gene expression values. The use of the MAD (a scale factor is used to consider the MAD as a consistent estimator for the estimation of data standard deviation), which computes the variability of the data from the median, makes the process more robust to outliers. In particular, a tuple probeset id, gene symbol, and the associated expression value are uniquely identified assuming that greater is the MAD higher is the goodness of the hybridization in the experiment. The code and dataset related to data preparation and pre-processing module have been made available at GitHub at <https://github.com/flaespo/NMF-for-GSE>.



**Figure 1.** Work flow of the NMF-based methodology for extraction of common genes between different tumor gene expression datasets.

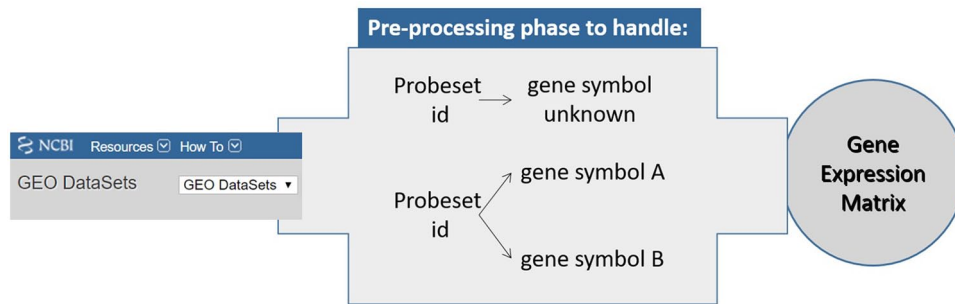


**Figure 2.** Possible cases supported by the pre-processing phase.

*Nonnegative matrix factorization for genetic data sets.* After data pre-processing is performed, most omic data sets can be represented as a matrix in which each element contains the measurement of a single molecule in a single experimental condition. In the case of expression data, the resulting high-dimensional data set is re-formulated as a numerical nonnegative matrix with rows being genes and columns representing samples, for example, tissues of various patients (as in this study), development stages, or treatments. This matrix is called “gene expression matrix” and its elements  $X_{ij}$  indicate the expression level of the gene  $i$  in the sample  $j$ . A main task in analyzing this matrix is to extract from it some knowledge about the underlying biological processes.

Nonnegative matrix factorization can be applied to reduce data dimensionality as it decomposes a gene expression matrix  $X$  by creating a user-defined number of new column features  $W(:,k)$ , ( $k=1, \dots, r$ ) called “metagenes,” which are linear combinations of the original samples set (eg, column vectors  $X(:,j)$ ) weighted with nonnegative coefficients

$$X(:,j) \approx \sum_{k=1}^r W(:,k)H_{kj},$$

for  $j=1, \dots, m$  and  $r \leq \min(m, n)$ . In this way, original data are explained by a sum of additive parts and so that intuitively biological entities and mechanisms can be naturally described with a signal that is either present or absent.

From an algebraic point of view, NMF finds 2 nonnegative matrices, the *metagenes matrix*  $W \in \mathbb{R}_+^{n \times r} = [W(:,1), \dots, W(:,r)]$  and the *metagene expression profiles matrix*  $H \in \mathbb{R}_+^{r \times m}$ , whose elements  $H_{ij}$  reveal the effect that the  $i$ th metagene  $W(:,i)$  has on the sample  $j$ , such that  $X \approx WH$ . It is worthy to observe that if the value  $H_{ij}$  is very small, then the corresponding metagene  $W(:,i)$  (having rows which are genes in  $X$ ) is useless in approximating that particular sample. The decomposition could be dually viewed as individuating metasamples (rather than metagenes) and groups of genes (rather than of samples) when the entries of  $W$  are taken into account.<sup>22,23</sup>

When NMFs are applied to produce clusters of genes, the rank value  $r$  is usually a priori set after trying different values, computing some quality measure of the results, and then choosing the best value according to the adopted quality criteria. In this article, however, we make use of some automatically suggested value accordingly a procedure described in

Del Buono and colleagues.<sup>8,23</sup> This procedure makes use of cophenetic coefficient, residuals sum of squares, dispersion curve, and consensus matrices to optimally address a proper rank value  $r$  for each gene expression matrix  $X$ .

Computationally, metagenes and expression profile values can be obtained solving a non-linear constrained optimization problem over the cone of nonnegative matrices

$$\min_{W \geq 0, H \geq 0} Div(X, WH) \quad (1)$$

where  $Div(X, WH)$  is any divergence measure which evaluates how well the low-dimensional matrix  $WH$  approximates  $X$ . In this article, the generalized Kullback-Leibler (KL) divergence

$$Div(X, WH) = \sum_{ij} \left( X_{ij} \log \left( \frac{X_{ij}}{(WH)_{ij}} \right) - X_{ij} + (WH)_{ij} \right)$$

is used, which corresponds to the maximum likelihood estimation under an independent Poisson assumption.<sup>24</sup> The minimization problem (1) for the KL divergence function is solved applying the following multiplicative update rules for  $W$  and  $H$ :

$$W_{ij} \leftarrow W_{ij} \frac{\sum_k (H_{jk} X_{ik}) / (WH)_{ik}}{\sum_k H_{jk}}$$

$$H_{ij} \leftarrow H_{ij} \frac{\sum_k (W_{ki} X_{kj}) / (WH)_{kj}}{\sum_k W_{ki}}$$

Because of the non-negativity constraint, solutions to NMF are only unique up to scaling and rotation, but appropriately scaling and rotating the columns of  $W$  and rows of  $H$  will not alter the overall matrix product  $WH$ . For this reason, what is of interest in practice is not the values of matrix elements, but their relative magnitudes in each column of  $W$  (or row of  $H$ ). Moreover, taking into account that more genes can participate in more than one biological process, it could be of some beneficial to investigate genes that have relatively large coefficients in each biological process.

To do this, the *gene.score* scoring method proposed in Kim and Park<sup>25</sup> has been adopted. This method computes a value *gene.score* ( $i$ ) value for each gene  $i$  in a metagene  $W(:, k)$  and selects those genes possessing *gene.score* value higher than a given threshold  $\tau$ . Particularly, the score threshold  $\tau$  is computed from the gene score vector itself as  $\tau = \hat{\mu} + 3\hat{\sigma}$ , being  $\hat{\mu}$  and  $\hat{\sigma}$  the median and the MAD of gene scores, respectively.

Metagenes in  $W$  contain the largest number of genes satisfying this empirical criterion and they can be considered as the most representative of the information hidden onto the gene expression data  $X$ . Observe that the metagenes NMF technique extracts are constrained by the dataset used to train them,

so a careful selection of datasets is essential: users need to choose those being broad enough to cover the relevant sources of variability.

*Gene Landscape Extraction procedure.* Referring to Figure 1, let  $X_i \in \mathbb{R}_+^{n_i \times m_i}$ ,  $i = 1, \dots, t$  be the gene expression matrices related to different biological experiments and let  $W_i \in \mathbb{R}_+^{n_i \times k_i}$  be the metagenes matrices obtained solving equation (1) for each  $X_i$  with an a priori rank  $k_i$ . In the proposed methodology, the constrained nonnegative optimization problem (1) have been solved via the *alternating method* in NMF R-package, with multiple executions and random initializations.<sup>8,20</sup>

To compare gene expression matrices derived from different tumor histotypes (in this work from their associated CAF cultures), the most representative metagene  $W_i(:, \tilde{k})$  is extracted from each gene expression matrix  $X_i$ . This metagene represents the  $\tilde{k}$ th column in the matrix  $W_i$ , which possesses the largest number of genes satisfying the *gene.score* criterium. These latter genes compose the gene-subsets automatically extracted from each tumor histotype.

To identify common genes among those extracted by different tumor histotypes, an intersection set operation was performed on the identification labels of genes  $W_i(:, \tilde{k})$  so that  $C = \bigcap_{i=1}^N W_i(:, \tilde{k})$  is a subset of gene-label common to each different tumor histotypes. It should be observed that the set of common genes  $C$  depends on the gene expression matrices initially selected.

Figure 3 provides a logical view of the Gene Landscape Extraction procedure, which represents the novel proposal to extract common genes from microarray matrices which differ in their sizes. Particularly, the microarray matrices  $X_i \in \mathbb{R}_+^{n_i \times m_i}$  obtained by the data preparation and pre-processing module from each tumor database are factorized by the NMF algorithm. This provides matrices  $W_i \in \mathbb{R}_+^{n_i \times r_i}$  and  $H_i \in \mathbb{R}_+^{r_i \times m_i}$ . Particularly, the rank values  $r_i$  used in the factorization process of the gene expression matrices used in this article are reported in Table 2. From each  $W_i$ , the most relevant metagene  $W_i(:, \tilde{k}_i)$  is automatically selected by the *gene.score* scoring method. These column vectors undergo the Gene Landscape Extraction procedure. It should be observed that which  $W_i(:, \tilde{k}_i)$  ( $i = 1, \dots, n$ ) differ in their number of rows (genes) and they are ordered to have the most representative information of the specific tumor histotype in their first components. Gene Landscape Extraction procedure uses intersection set operations to identify labels of genes in each  $W_i(:, \tilde{k}_i)$ , which are common to each different tumor histotypes.

### Functional and visual analysis

The obtained subset of genes is then analyzed by integrative bioinformatic tools, that is, the WebGestalt tool,<sup>26</sup> to discover the role they cover into the biological process under investigation.

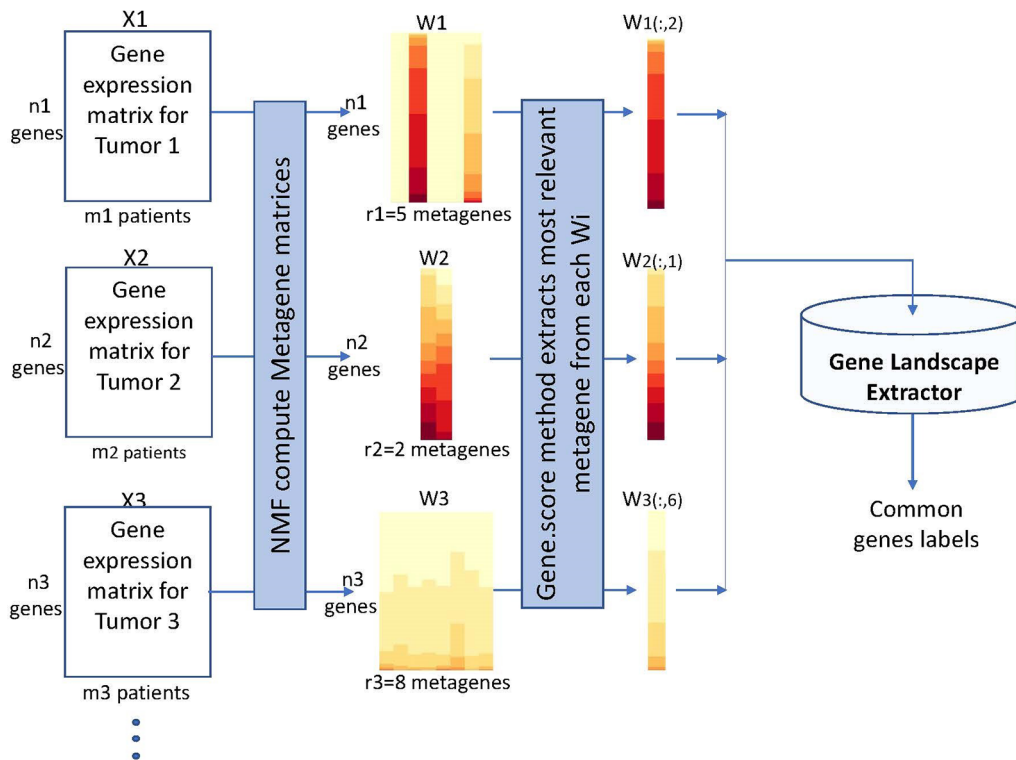


**Figure 3.** Logical view of the gene landscape extraction. Preprocessed expression data matrices related to 3 different tumors ( $X_1, X_2, X_3$ ) are factorized by the NMF algorithm and corresponding metagenes matrices  $W_i$  ( $i = 1, 2, 3$ ) are taken into considerations. Gene.score scoring method selects the most relevant metagenes ( $W_i(:, \tilde{k}_i)$ ), ( $i = 1, 2, 3$ )  $i$ , which undergo the Gene Landscape Extraction procedure. This latter uses an intersection set operation to identify labels of genes common to each different tumor histotypes. The extracted subset of gene-labels is then sent to the functional and pathway analyses.

This module performs either functional and pathway enrichment analysis of the genes in  $C$ . Some graphical utilities were also added to better visualize the results provided. For instance, a variation of the UpSet plot is used to highlight most frequent genes and the pathway they belong to. The novelty of this representation with respect to the standard UpSet plot is the possibility of drawing the height and the width of each bar. To quantify the intersection between each pathway, the bars in the plot are proportional to the relative frequencies and to the number of genes selected in each set of pathway. This graphical representation was used in the following.

### Application to the Analysis of Gene Expression Profiles of CAFs

In this section, we sequentially applied the main modules of the proposed methodology for automatically extract genes from gene expression profiles of CAFs.

Fibroblasts are the most heterogeneous and abundant population of mesenchymal cells in the TME,<sup>27</sup> but their precise functional role in tumor is not fully understood yet.<sup>13</sup> During initial phases of oncogenesis, fibroblasts are activated giving rise to fibroblasts associated with the tumor (CAF), which play a key role in generating a specific extracellular matrix (ECM) in TME.<sup>28</sup> The kinetics of changes in CAF actions might be different in the various types of tumor, partly because of organ-specific transcriptomic profiles of resident fibroblasts<sup>29</sup> and

partly as different subtypes of CAF could exert distinct paracrine actions affecting specific tumor oncogenesis.<sup>14,15</sup> Currently, either the number of CAF subpopulations present in the tumor stroma and the role assumed by the presence of an individual population or different cell types into tumor initial development stages are unknown.<sup>6,16</sup> Some characteristics distinguish CAFs from quiescent fibroblasts as, for instance, metabolic adaptations supporting their need for advanced proliferation and biosynthesis activities.<sup>13</sup> Furthermore, a potentially controversial area of research on CAFs is focused on their origin. In fact, to define and identify origin of fibroblasts, it is fundamental to consider that CAFs are “activated fibroblasts” and unlike the non-activated (quiescent) fibroblasts residing in the tissue, they are an expansion of the cell population proliferating “in situ” or are recruited in the tumor.<sup>30</sup> Recruitment of BM mesenchymal stem cells, differentiation from adipose stem cells, or conversion from endothelial cells through an epithelial-endothelium-mesenchymal transition process are potential origins of CAFs.<sup>13</sup> However, the best documented source of CAFs is the activation of “normal” resident fibroblasts which, with their heterogeneity, imply the existence of different subsets. This heterogeneity may reflect the variability with respect to phenotypic state of both cell and tissue of origin and therefore also the reporting mediators and the mechanisms to be activated.<sup>14,31</sup> In fact, CAFs can be distinguished from other types of cells within the tumor by means of exclusion criteria

defined by their morphological characteristics and by a lack of expression of non-mesenchymal markers, such as those expressed by endothelial, epithelial, immune, and neuronal cells even if none of these has an absolute specificity.<sup>32</sup> A challenging aspect in CAFs studies is the precise definition of heterogeneous CAF populations in distinct phases of tumor progression through markers informing on their functions.<sup>6,33</sup>

In this study, we used the proposed NMF-based gene extractor methodology to investigate CAFs heterogeneity to identify the possible presences of genes, which can be biomarkers and characterize activated fibroblast phenotype. Gene expression profiles of CAFs belonging to primary cultures of 3 distinct solid tumor histotypes from patients (ie, colon of endodermal origin, breast carcinoma of ectodermal origin and ovary of mesodermal origin) were considered. Moreover, we also verified the existence of common genes among CAF gene expression profiles of selected solid tumors and those of BM of patients with multiple myeloma (MM)<sup>6</sup> and MGUS.<sup>17</sup>

#### Identification of CAF populations and download of transcriptomic profiles

International Agency for Research on Cancer (IARC) estimates 18.1 million (17.0 million excluding non-melanoma skin cancer) new cancer cases in 2018, causing about 9.6 million of deaths (9.5 million excluding non-melanoma skin cancer).<sup>34</sup>

For studying the heterogeneous CAF population, which represents the most abundant cellular component of the TME, representative tumor histotypes with high rate of mortality have been selected: colon carcinoma, breast cancer, ovarian cancer, and MM. The gene expression profiles of CAFs were downloaded from the Gene Expression Omnibus database (GEO) NCBI (a functional public genomic database that supports the submission of MIAME-compliant data) directly from the original publications of each series ([https://www.ncbi.nlm.nih.gov/geo/query/acc.cgi?acc=GEO\\_series](https://www.ncbi.nlm.nih.gov/geo/query/acc.cgi?acc=GEO_series)).<sup>35</sup> Data sets were selected according to the following standards: (a) the GEO platform (GPL) and (b) the number of samples with labels to identify the fibroblasts associated with the tumor (being  $\geq 7$  the total amount of samples for each representative cancer). Table 1 reports GSE series, bibliographical references, GPL, GSM labels, and the numbers of samples and expressed genes for each data set and finally, the rank values adopted to obtain NMF decomposition.

## Results

### Functional analysis

Nonnegative matrix factorization-based methodology identified a subset of 108 genes common to colon, breast, and ovarian tumors. The biological analysis these genes underwent during the functional and visual analysis phase is detailed in the following. Table 2 summarizes the Gene Ontology functional analysis, Table 3 the Pathway enrichment analysis,

whereas in Table 4 are detailed all the 108 genes that underwent the biological analysis. Furthermore, considering that the population of CAF in TME is also recruited by the BM, contributing with important percentages on the total CAF population, the gene expression profiles of primary CAFs of MGUS and MM were used to select the presence of genes, which are common among the CAF “in situ” of the analyzed tumors and CAF recruited by the BM.

**Gene Ontology functional analysis.** Gene Ontology (GO) was used to classify common genes; classification is obtained according to biological processes, molecular functions, or cellular components. Some genes were identified as related to processes significantly representative of the immune response and associated with nucleic acids metabolism. In particular,

- 23 (21.3%) and 13 (12%) genes are involved in the “immune response” and “innate immune response” biological processes with false discovery rate (FDR) values 0.1615 and 0.3362, respectively. *ABCE1*, *ANXA1*, *APOBEC3B*, *APOBEC3G*, *BST2*, *CFH*, *FBXO9*, *HLA-DQA1*, *HLA-DQB1*, *JCHAIN*, *MATR3*, *TRIM14*, and *TRIM59* are genes common to both processes. On the contrary, *DNAJC13*, *ENPP2*, *FOS*, *NBN*, *PGRMC1*, *PNP*, *RIF1*, *ROCK1*, *TAP2*, and *TGFBR3* are genes characterizing “immune response” processes, but which do not participate in the “innate immune response.”
- 17 genes (15.7%) are involved in the catabolic “organonitrogen compound catabolic process” with an FDR value of 0.2571; they are *AOX1*, *APOBEC3B*, *APOBEC3G*, *AZIN1*, *CDH1*, *ENPP2*, *FBXO9*, *GPC6*, *HERC2*, *HNMT*, *MBD4*, *PNP*, *PSMB9*, *ROCK1*, *SYNPO2*, *UBA6*, and *TRIM2*. The remaining biological processes that characterize GO share the above-mentioned genes.

The 3 major biological processes “immune response,” “innate immune response,” and “organonitrogen compound catabolic process” characterizing the GO share 3 genes: *APOBEC3B*, *APOBEC3G*, and *FBXO9*. The *APOBEC3B* and *APOBEC3G* genes belong to members of the cytidine deaminase gene family. All the components of the APOBEC family, with the exception of *APOBEC2* and *APOBEC4*, are able to convert, in single-stranded DNA, the cytosine through a deamination reaction in uracil.<sup>41-43</sup>

The *FBXO9* gene encodes a member of the F-box family of proteins. F-box proteins are one of the 4 subunits of the ubiquitin protein ligase complex called SCF (SKP1-cullin-F-box), which works in phosphorylation-dependent ubiquitination.<sup>44</sup> Furthermore, FBXO9 manifests the effects on mTOR by directing cells toward cellular survival when growth factors become limiting. These studies suggest that FBXO9 could act as an oncogene.<sup>45</sup>

The genes that differentiate the “immune response” from the “innate immune response” are *FOS*, *TGFBR3*, *ROCK1*,

**Table 1.** Dataset information: GSE series used, bibliographical references, GEO platforms (GPL570, GPL6244, and GPL2136 indicate Affymetrix Human Genome U133 Plus\_2.0 Array, Affymetrix Human Gene 1.0 ST Array, and Micro-CRIBI Human Oligo Array [Operon V2.0], respectively), fibroblast sample labels, representative cancer, number of genes, number of samples, and NMF rank value  $r_i$  used.

GSE	REF.	GPL	GSM LABELS	REPRESENTATIVE CANCER	NO. GSM	NO. GENES	$r_i$
GSE51257	<sup>36</sup>	GPL6244	Cancer-associated fibroblast	Colon carcinoma	4	20 304	2
GSE30292	<sup>37</sup>	GPL570	Cancer-associated fibroblast	Colon carcinoma	3	22 189	3
GSE75333	<sup>38</sup>	GPL570	Carcinoma-associated fibroblast	Breast carcinoma	3	22 189	2
GSE20086	<sup>39</sup>	GPL570	Carcinoma-associated fibroblast	Breast cancer	6	22 189	2
GSE40595	<sup>40</sup>	GPL570	Ovarian Cancer stroma	Ovarian cancer	10	22 189	2
GSE24990	<sup>6</sup>	GPL2136	Active multiple myeloma	MM	18	21 520	8
			MGUS	MGUS			5

**Table 2.** Gene ontology functional analysis: based on the parameters used, 10 categories are identified as enriched categories and all are shown in this table.<sup>9</sup>

GENE SET	DESCRIPTION	SIZE	EXPECT	RATIO	P VALUE	FDR
GO:0006955	Immune response	1919	9.0964	2.5285	.00001777	0.1615
GO:1901565	Organonitrogen compound catabolic process	1240	5.8778	2.8922	.00005655	0.2571
GO:0042454	Ribonucleoside catabolic process	22	0.1043	28.7680	.00014794	0.3362
GO:0009164	Nucleoside catabolic process	34	0.1612	18.6140	.00055180	0.8992
GO:0072529	Pyrimidine-containing compound catabolic process	38	0.1801	16.6550	.00076738	0.8992
GO:0048525	Negative regulation of viral process	88	0.4171	9.5892	.00080637	0.8992
GO:1901658	Glycosyl compound catabolic process	44	0.2086	14.3840	.00118040	0.8992
GO:0006216	Cytidine catabolic process	11	0.0521	38.3570	.00118690	0.8992
GO:0009972	Cytidine deamination	11	0.0521	38.3570	.00118690	0.8992

The parameters for the analysis of enrichment are minimum number of IDs in the category: 5; maximum number of IDs in the category: 2000; FDR method: BH; level of significance: Top 10.

**Table 3.** Pathway enrichment analysis: based on the parameters used, 10 categories are identified as enriched categories and all are shown in this table.<sup>9</sup>

GENE SET	DESCRIPTION	SIZE	EXPECT	RATIO	P VALUE	FDR
P00053	T cell activation	75	0.3972	7.5533	.00617920	0.3686
P00032	Insulin IGF pathway mitogen-activated protein kinase kinase MAP kinase cascade	29	0.1536	13.0230	.00964300	0.3686
P06959	CCKR signaling map	172	0.9109	4.3915	.00978500	0.3686
P00047	PDGF signaling pathway	125	0.6620	4.5320	.02499200	0.6789
P02723	Adenine and hypoxanthine salvage pathway	6	0.0318	31.4720	.03139100	0.6789
P00010	B cell activation	58	0.3071	6.5115	.03604900	0.6789
P00031	Inflammation mediated by chemokine and cytokine signaling pathway	200	1.0591	2.8325	.08217900	1.0000
P00002	Alpha adrenergic receptor signaling pathway	23	0.1218	8.2101	.11549000	1.0000
P00004	Alzheimer disease-presenilin pathway	112	0.5931	3.3720	.11570000	1.0000
P00041	Metabotropic glutamate receptor group I pathway	24	0.1271	7.8681	.12022000	1.0000

The parameters for the analysis of enrichment are minimum number of IDs in the category: 5. Maximum number of IDs in the category: 2000; FDR method: BH; and level of significance: top 10.

**Table 4.** List of the 108 genes common to colon, breast, and ovarian tumors identified by NMF-based methodology described in this article.

CDH1	EFEMP1	IGLC1	MATR3	RARRES1	FANCL	JCHAIN	PNN	GAGE12F
GAGE2A	GAGE12H	GAGE12E	GAGE2D	GAGE8	GAGE12J	GAGE12G	GAGE13	GAGE2E
GAGE6	GAGE5	GAGE4	GAGE2C	GAGE1	BEX4	NFYB	ITGB8	IGHV4-31
IGHM	IGHG1	IGLV1-44	ANXA1	COL14A1	BST2	SLC16A14	GPC6	UBA6
CKAP2	MGARP	BCL2L13	HLA-DQB1	ZNF644	DMD	HOXD8	FOS	SLC40A1
SLC39A8	ETNK1	PMS1	PSMB9	RCBTB1	EEA1	NBN	MAP7	TGFBR3
ENPP2	DNAJC13	RBM25	RSRC2	SPARCL1	CFH	INS-IGF2	IGF2	HNRNPA2B1
ANKRD28	EIF4E2	MBD4	TRIM14	CP	DZIP3	IFT80	TAP2	ITPR1
HNMT	TTC14	LMBRD2	MINA	TRIM59	IGKC	AZIN1	AOX1	PRPF4B
SYNPO2	FBXO9	ZNF277	APOBEC3B	TRIM2	GTF2H2B	NR3C1	CHN2	ROCK1
HLADQA1	RIF1	ABCE1	APOBEC3G	KIF26B	SLC2A13	PCMTD2	ZNF655	HERC2
RARRES3	FLI1	ZDHHC21	PNP	SIK1	SHROOM3	PGRMC1	LINC01116	KIAA1109

*TAP2*, and *NBN* that encode essentially binding proteins; proteins encoded by *ENPP2*, *TGFBR3*, *TAP2*, and *PNP* genes have specific biological properties linked to immunity, while *FOS*, *NBN*, and *PNP* genes encode proteins that can be associated with pharmacological responses. The biological processes of the “immune response” and “organonitrogen compound catabolic process” have in common the genes *ENPP2*, *PNP*, and *ROCK1*. The *ENPP2* gene encodes a protein that functions both as a phosphodiesterase and as a phospholipase, which catalyzes the production of lysophosphatidic acid (LPA) in extracellular fluids. Lysophosphatidic acid evokes similar responses to growth factors including stimulation of cell proliferation and chemotaxis. Autotaxin (*ENPP2* or *ATX*) was originally identified as an “autocrine motility factor” for tumor cells and has angiogenic properties and its expression is upregulated in different types of carcinomas.<sup>46</sup> The *PNP* gene encodes an enzyme that reversibly catalyzes the phosphorolysis of purine nucleosides, one of its deficits determines a defective immunity of T cells (cell-mediated) but also the immunity of B cells and the antibody responses may be involved.<sup>47</sup>

The *ROCK1* gene encodes a serine/threonine kinase protein that is activated when bound to the Rho-bound GTP form. The small GTPase Rho regulates the formation of focal adhesion and fibroblast stress fibers, as well as the adhesion and aggregation of platelets and lymphocytes.<sup>48,49</sup> The biological process “organonitrogen compound catabolic process” consists largely of binding proteins (*TRIM2*, *MBD4*, *UBA6*, *CDH1*, *PSMB9*, and *HERC2*), with properties of ligase and ubiquitinating activity (*TRIM2*, *UBA6*, and *HERC2*). Among the genes belonging to GO, some are associated with events related to the epithelial-to-mesenchymal transition (EMT; *TGFBR3*, *CDH1*, and *FOS*), others to cellular transport through extracellular and intracellular membranes (*TAP2* and *DNAJC13*) and to the immortalization process (*RIF1*). The *TβRIII*, independent of its TGF-β

co-receptor function, regulates the canonical signaling of Wnt3a. Therefore, *TβRIII* plays the role of mediator of TGF-β superfamily signaling during tumor progression.<sup>50,51,52</sup> The *CDH1* protein belongs to the cadherine super-family and is a calcium-dependent cell adhesion protein. Changes in function of this gene or loss are thought to contribute to EMT, proliferation, invasion, and/or metastasis.<sup>53,54</sup> *FOS* proteins have been implicated as regulators of cell proliferation, differentiation, and transformation.<sup>55</sup> Proteins encoded by the *TAP2* and *DNAJC13* genes are particularly involved in cellular transport through extracellular and intracellular membranes. The *TAP* protein is a member of the super-family of the ATP (ABC) cassette transporters, in particular the *MDR/TAP* subfamily involved in multidrug resistance and is also involved in antigen presentation.<sup>56</sup> The *DNAJC13* gene encodes *Dnaj* proteins that are combined with heat-shock proteins by stimulating ATP hydrolysis. In particular, *DNAJC13* is associated with the *Hsc70* protein and plays a role in clathrin-mediated endocytosis and in post-endocytic transport mechanisms.<sup>57</sup> Finally, the *RIF1* gene encodes a protein that shares the homology with the yeast telomere binding protein, *Rap1* interaction factor. This protein locates in aberrant telomeres that may be involved in DNA repair, altering cell growth and proliferation.<sup>58</sup>

**Pathway enrichment analysis.** PANTHER reference database (Protein Analysis Through Evolutionary Relationships) was used to evaluate with the WebGestalt tool the selected 108 genes during the pathway enrichment analysis. The selected 10 pathways were reported in Table 3. The first 6 pathways are characterized by an FDR below 1 and a *P* value <.05. The 10 genes (9.25%) included in the pathways are as follows:

- *ITPR1* gene is present in 7 out of 10 pathways: *T cell activation*, *CCKR signaling map*, *PDGF signaling pathway*, *B cell activation*, *inflammation mediated by chemokine*



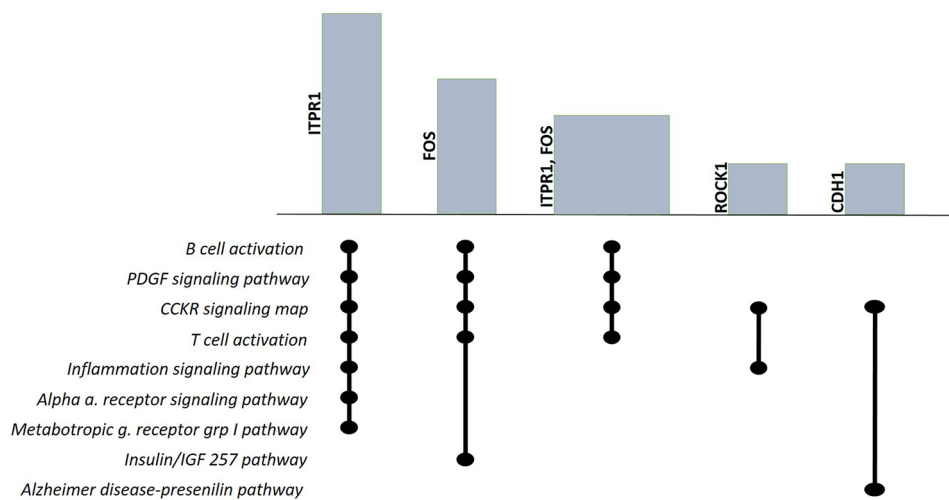


**Figure 4.** Variation of the UpSet plot<sup>59</sup> of the most frequent genes: *ITPR1*, *FOS*, *ROCK1*, and *CDH1*. The intersection between *ITPR1* and *FOS* genes is also plotted to emphasize the pathway they belong to, commonly.

and cytokine signaling pathway, alpha adrenergic receptor signaling pathway, and metabotropic glutamate receptor group I pathway.

- *FOS* gene is present in 5 out of 10 pathways: *T cell activation pathways*, *insulin/IGF pathway-mitogen-activated protein kinase kinase/MAP kinase cascade*, *CCKR signaling map*, *PDGF signaling pathway*, and *B cell activation*.
- *CDH1* gene. It is present in 2 out of 10 pathways: *CCKR signaling map* and the *Alzheimer disease-presenilin pathway*.
- *ROCK1* gene. It is present in 2 out of 10 pathways: the *CCKR signaling map* and *inflammation mediated by chemokine and cytokine signaling pathway*.
- *HLA-DQA1* gene is in *T cell activation*;
- *IGF2* gene is in *insulin/IGF pathway-mitogen-activated protein kinase kinase/MAP kinase cascade*;
- *FLI1* gene is in *PDGF signaling pathway*;
- *PNP* gene is in *adenine and hypoxanthine salvage pathway*;
- *COL14A1* gene is in *inflammation mediated by chemokine and cytokine signaling pathway*;
- *TRIM2* gene is in *Alzheimer disease-presenilin pathway*.

Figure 4 illustrates the most frequent genes and the pathway they belong to using a variation of the UpSet plot. Height and width of bars are proportional to the relative frequencies and to the number of genes selected in each set of pathway.

The *FOS*, *CDH1*, *ROCK1*, and *PNP* genes have been discussed in the GO section. Among the genes not discussed in the GO (Figure 4), we have *ITPR1*, *HLA-DQA1*, *IGF2*, *FLI1*, *COL14A1*, and *TRIM2*. The presence of the *ITPR1* gene in 7 pathways demonstrates the centrality of this protein, which is an intracellular receptor for inositol 1,4,5-trisphosphate that after stimulation mediates the release of calcium from the endoplasmic reticulum. The InsP3/Ca<sup>2+</sup> pathway works to regulate

many cellular processes. The versatility and universality of this pathway is based on 2 main operating modes: providing the Ca<sup>2+</sup> signal playing a direct role in the regulation of different processes such as cell proliferation, secretion, metabolism, fertilization, and contraction of smooth muscle. The second modality is to modulate the activity of various excitable cells.<sup>60,61</sup> The *IGF2* and *FLI1* *COL14A1* genes are regulators in the morphogenesis process, *IGF2* is a growth factor that performs hormonal activity by binding to the insulin receptor, and the *COL14A1* gene is involved in fibrillogenesis and creates bridges with the collagen of the ECM; the *FLI1* gene is a transcription factor of the ETS family and regulates the expression of oncogenes, tumor suppressor genes, and some genes related to angiogenesis, invasion, and metastasis.<sup>62-64</sup> Furthermore, the *ITPR1* gene (Figure 4) shares 4 fundamental pathways in the immune response with the *FOS* gene, confirming that the action of the *ITPR1* gene as an intracellular receptor for inositol 1,4,5-trisphosphate determines inputs that also involve *FOS* protein (component of the transcription factor AP1) in processes associated with immune control. Finally, the *HLA-DQA1* gene plays a central role in the immune system by presenting peptides derived from extracellular proteins and is found in several cell types<sup>65</sup> and the *TRIM2* gene encodes a protein that is located close to the cytoplasmic filaments and functions as E3-ubiquitin ligase. Furthermore, it has been widely reported that the proteins of the TRIM family play a large role in the biological processes of autophagy, inflammation, immunity, and tumor.<sup>66</sup> The selected pathways provide signals for T and B lymphocytes and signals for cytokine and chemokine-mediated inflammatory processes as the GO has shown by selecting biological events related to the immune response. Moreover, we observe the involvement of growth factor pathways such as PDGF and IGF, alpha adrenergic and glutamate receptors, as well as hormones such as cholecystokinin and gastrin all together demonstrate that CAFs become sensitive to the conditions of the TME.

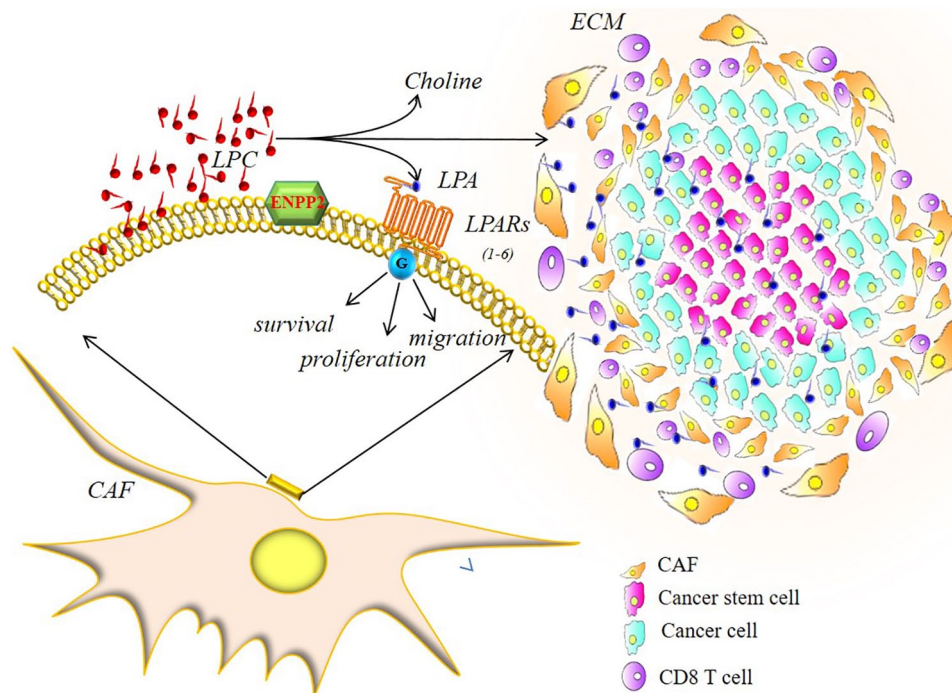


**Figure 5.** ECM (extracellular matrix). The ENPP2 protein, common to the CAFs of the 4 tumors analyzed, catalyzes the LPC hydrolysis in LPA, activating its local LPA receptors and the corresponding G proteins. LPA signals through its receptors to induce proliferation, survival, and invasion in tumor cells and cancer stem cells. LPA signaling also induces the recruitment of CAFs cells and a wide range of cellular responses and also reduces the cytotoxic immune response.

*Identification of genes common among CAFs in colon, breast, and ovarian tumors and MGUS.* The subgroup of the 108 genes obtained from the intersection of genes belonging to the representative metagenes of the CAF gene profiles related to colon, ovary, and breast tumors has been intersected with the metagene representative of the MGUS CAF gene profiles. The data sets containing gene subgroups are made available as supplement materials.

The profile intersection produced a subgroup of 9 genes: *ANXA1*, *EIF4E2*, *ETNK1*, *GPC6*, *HLA-DQA1*, *IFT80*, *IGHM*, *PMS1*, and *UBA6*. In this subgroup, the *ANXA1* gene has a leading role, as the *ANXA1* protein has demonstrated complex roles in many different cellular functions, such as inflammation, regulation of proliferation, membrane interactions, phagocytosis, and cellular apoptosis. In particular, the anti-inflammatory activity is determined by the inhibition of the activity of cytosolic phospholipase A2 (cPLA2) and of cyclooxygenase 2 (COX-2).<sup>67</sup> The alterations of *ANXA1* could reveal important functions in tumorigenesis and in the development of cancer. Among the other genes belonging to this subgroup, the *IFT80* and *GPC6* genes are responsible for the regulation of the non-canonical Wnt pathway, a pathway that organizes the cytoskeleton and the planar polarity of the cell, regulating its shape, especially *IFT80* is essential in differentiation processes.<sup>68,69</sup> The *UBA6*, *PMS1*, and *EIF4E2* genes are involved in the process of ubiquitination, repair, and activation of protein synthesis in a hypoxic environment. In particular, the ubiquitination pathways specifically initiated by *UBA6* can create a suppressive barrier against the

critical steps of carcinogenesis such as loss of polarity, resistance to anoikis, and epithelial-mesenchymal transition (EMT).<sup>70,71</sup> Finally, the *IGHM*,<sup>72</sup> *HLA-DQA1*,<sup>73</sup> and *ETNK1*<sup>74</sup> genes are involved in the immune response.

*Identification of common genes among CAFs in colon, breast, ovary, and MM tumors.* Similarly, the subgroup of the 108 genes obtained from the intersection of genes belonging to the metagenes representative of the gene profiles of CAFs related to colon, ovary, and breast tumors was intersected with the representative metagene of the gene profiles of MM CAF. The profile intersection produced only one gene: ENPP2 (ectonucleotide pyrophosphatase/phosphodiesterase or autotaxin-ATX; illustration is provided in Figure 5). Autotaxin is an exo-enzyme originally identified as an autocrine motility factor of the cancer cell. ATX is unique among nucleotide pyrophosphatase/phosphodiesterase (NPPs) as it functions primarily as lysophospholipase D, converting lysophosphatidylcholine into the lipid mediator of LPA. Lysophosphatidic acid acts on specific G protein-coupled receptors to elicit a wide range of cellular responses, ranging from cell proliferation and migration to the production of cytokines.<sup>75,76</sup>

## Discussion

The transcriptome analysis of colon, ovary, and breast tumors selected a subgroup of 108 genes by NMF-based methodology identifying a CAF phenotype with morphological and functional characteristics regardless of embryonic origin. In fact,

the *APOBEC3B* and *APOBEC3G* genes confer susceptibility to mutations that determine the heterogeneity of CAF. The *TGFBR3* genes, *CDH1*, determine the plasticity that leads to EMT, an event that demonstrates the active state of fibroblasts, to which we also associate the genes *ROCK1* and *COL14A1*. In addition, in TME, the functional role of CAFs has shown the involvement of growth factor pathways such as PDGF and IGF, alpha adrenergic and glutamate receptors, as well as hormones such as cholecystokinin and gastrin and the ability to activate cells linked to immune response such as T lymphocytes and B lymphocytes (*HLA-DQA1*, *PNP*, and *ENPP2*). All these events are controlled by transcription factors (*FOS*, *FLI1*), by the regulation of transport mechanisms (*TAP2*, *DNAJC13*), by transduced signals (*ITPR1*), and by degradation processes (*FBXO9*, *TRIM2*). The genes obtained from the intersection of the subgroup of the 3 tumor histotypes with the MGUS metagene consolidate the hypothesis of a “primitive” recruited CAF, adaptable to a hypoxic TME (*EIF4E2*) and which has assumed the role of barrier (*IFT80*, *GPC6*), with an anti-inflammatory action (*ANXA1*, *UBA6*), of immunological control and repair with *HLA-DQA1* and *PMS1* proteins. The intersection of the subgroup of the 3 tumor histotypes with the MM metagene primarily drastically reduces the number of common genes and delivers to the analysis only the *ENPP2* gene, which identifies a phenotype of pro-inflammatory CAF. Therefore, the CAF recruited from the BM, coming from MGUS, a non-pathological condition, could assume a barrier function toward the tumor, and instead the primary fibroblasts from MM, they represent a pro-inflammatory CAF phenotype which makes TME even more pro-tumorigenic probably in favor of the expansion of the fibroblastic clone which proliferates “in situ.” In fact, the ATX-LPA axis that induces LPA production in many tumors is overexpressed and affects different phases of the disease, starting from inflammation, development, and progression of the tumor. The results show that the CAF phenotype that emerges in the 3 tumor histotypes analyzed is characterized by the action of genes that modulate heterogeneity (*APOBEC3B*, *APOBEC3G*). The different subpopulations generated have a common line that, regardless of the starting tissue, is given by the genes: *CDH1*, *COL14A1*, *DNAJC13*, *ENPP2*, *FBXO9*, *FLI1*, *HLA-DQA1*, *ITPR1*, *PNP*, *ROCK1*, *TAP2*, *TGFBR3*, and *TRIM2*. Therefore, the genes just listed could be used as biomarkers, as well as the CAF genes recruited by the BM, in particular the *ENPP2* gene.

## Conclusions

We proposed a mathematical methodology based on NMF, which has been originally assembled for automatically extracting common genes from different gene expression data. This computational mechanism has 2 main features: (1) through NMF method, metagenes which are the most representative of the information embedded into different tumor gene expression

data are extracted; (2) through basic mathematical set operations (implemented into the gene landscape extraction module), genes common to different tumor histotypes are selected. These genes can then be easily analyzed from a biological point of view through the functional and the visualization approaches based on the WebGestalt tool, which integrates the computational mechanisms.

The proposed mechanism demonstrated its usefulness in identifying genes which could be helpful to better understand the molecular mechanisms behind the activation of fibroblasts and their role in tumor progression. Different CAF subpopulations in the TME can be distinguished from one another by the expression of one or more specific markers. In general, CAFs have the common function of altering the TME; in fact, once activated, fibroblasts synthesize and deposit ECM components, release chemokines and cytokines in the stroma, and generate tension forces at the tissue level through their cytoskeletons, all are requirements key for tissue remodeling. The multifaceted nature of CAF is therefore linked to the TME in which the various pathways are activated as the mechanism based on the TGF- $\beta$  signal and/or the bidirectional communication between the fibroblasts and the tumor cells.

Our study has shown that, even if there is phenotypic heterogeneity of CAF (*APOBEC3B*, *APOBEC3G*), in tumors of different embryonic origin, there are common biomarkers, characterizing the phenotype of activated fibroblasts. Furthermore, we were able to identify a phenotype of CAF as an anti-inflammatory (*ANXA1*, *UBA6*) likely associated with the first stages of tumor transformation and subsequently pro-inflammatory with the *ENPP2* gene, which activates the ATX-LPA axis, which is responsible for numerous events involved in the development and progression of the tumor. Therefore, the “in situ” fibroblasts, in the tumors studied, acquire a more heterogeneous phenotype because they are induced by genes that favor heterogeneity and by the stimuli coming from the TME associated with the different tumor histotypes. Naturally, this result constitutes a further aid to the difficult challenge to characterize the CAF, to counteract their action in the TME, which allows to be able to improve the clinical-therapeutic approaches.

## Author Contributions

AB designed the research and analysed the numerical results. NDB and FE performed the mathematical analysis and the data preprocessing. FE designed and implemented the framework modules. AB, NDB and FE drafted and reviewed the manuscript and did the critical revision of the final version of the paper. All the authors read and approved the manuscript in its final form.

## ORCID iDs

Flavia Esposito  <https://orcid.org/0000-0002-2791-9610>

Angelina Boccarelli  <https://orcid.org/0000-0002-9514-2022>

## Supplemental material

Supplemental material for this article is available online.

## REFERENCES

- Zhang S, Liu CC, Li W, Shen H, Laird PW, Zhou XJ. Discovery of multi-dimensional modules by integrative analysis of cancer genomic data. *Nucleic Acids Res.* 2012;40:9379-9391. doi:10.1093/nar/gks725
- Kim PM, Tidor B. Subsystem identification through dimensionality reduction of large-scale gene expression data. *Genome Res.* 2003;13:1706-1718.
- Frigyesi A, Hoglund M. Non-negative matrix factorization for the analysis of complex gene expression data: identification of clinically relevant tumor subtypes. *Cancer Inform.* 2008;6:275-292.
- Carrasco D, Tonon G, Huang Y, et al. High-resolution genomic profiles define distinct clinico-pathogenetic subgroups of multiple myeloma patients. *Cancer Cell.* 2006;9:313-325. doi:10.1016/j.ccr.2006.03.019.
- Esposito F, Gillis N, Del Buono N. Orthogonal joint sparse NMF for microarray data analysis. *J Math Biol.* 2019;79:223-247.
- Boccarelli A, Esposito F, Coluccia M, Frassanito MA, Vacca A, Del Buono N. Improving knowledge on the activation of bone marrow fibroblasts in mgus and mm disease through the automatic extraction of genes via a nonnegative matrix factorization approach on gene expression profiles. *J Transl Med.* 2018;16:217. doi:10.1186/s12967-018-1589-1.
- Brunet JP, Tamayo P, Golub TR, Mesirov JP. Metagenes and molecular pattern discovery using matrix factorization. *Proc Natl Acad Sci U S A.* 2004;101:4164-4169.
- Del Buono N, Esposito F, Fumarola F, et al. Breast cancer's microarray data: pattern discovery using nonnegative matrix factorizations. In: Pardalos PM, Conca P, Giuffrida G and Nicosia G eds. *International Workshop on Machine Learning, Optimization and Big Data.* Berlin, Germany: Springer; 2016, 281-292.
- Liao Y, Wang J, Jaehng EJ, Shi Z, Zhang B. WebGestalt 2019: gene set analysis toolkit with revamped UIS and APIS. *Nucleic Acids Res.* 2019;47:W199-W205.
- Fujita N, Mizuarai S, Murakami K, Nakai K. Biomarker discovery by integrated joint non-negative matrix factorization and pathway signature analyses. *Sci Rep.* 2018;8:9743. doi:10.1038/s41598-018-28066-w.
- Zi Y, George M. A non-negative matrix factorization method for detecting modules in heterogeneous omics multi-modal data. *Bioinformatics.* 2015;32:1-8. doi:10.1093/bioinformatics/btv544.
- Mazandu GK, Chimusa ER, Rutherford K, et al. Large-scale data-driven integrative framework for extracting essential targets and processes from disease-associated gene data sets. *Brief Bioinform.* 2017;19:1141-1152. doi:10.1093/bib/bbx052.
- LeBleu VS, Kalluri R. A peek into cancer-associated fibroblasts: origins, functions and translational impact. *Dis Model Mech.* 2018;11:dmm029447. doi:10.1242/dmm.029447.
- Costa A, Kieffer Y, Scholer-Dahirel A, et al. Fibroblast heterogeneity and immunosuppressive environment in human breast cancer. *Cancer Cell.* 2018;33:463-479. doi:10.1016/j.ccell.2018.01.011.
- Wagner EF. Fibroblasts for all seasons. *Nature.* 2016;530:42-43. doi:10.1038/530042a.
- Franco OE, Shaw AK, Strand DW, et al. Cancer associated fibroblasts in cancer pathogenesis. *Semin Cell Dev Biol.* 2010;21:33-39. doi:10.1016/j.semcdb.2009.10.010.
- van de Donk NW, Mutis T, Poddighe PJ, Lokhorst HM, Zweegman S. Diagnosis risk stratification and management of monoclonal gammopathy of undetermined significance and smoldering multiple myeloma. *Int J Lab Hematol.* 2016;38:110-122. doi:10.1111/ijlh.12504.
- Huber W, Carey VJ, Gentleman R, et al. Orchestrating high-throughput genomic analysis with bioconductor. *Nat Methods.* 2015;12:115-121.
- Davis S, Meltzer PS. GEOquery: a bridge between the gene expression omnibus (geo) and bioconductor. *Bioinformatics.* 2007;23:1846-1847.
- Gaujoux R, Seoighe C. A flexible R package for nonnegative matrix factorization. *BMC Bioinform.* 2010;11:367. doi:10.1186/1471-2105-11-367.
- Knudsen S. *Guide to Analysis of DNA Microarray Data.* New York, NY: John Wiley & Sons; 2004.
- Del Buono N, Pio G. Non-negative matrix tri-factorization for co-clustering: an analysis of the block matrix. *Information Sciences.* 2015;301:13-26. doi:10.1016/j.ins.2014.12.058.
- Casalino G, Castiello C, Del Buono N, et al. Q-matrix extraction from real response data using nonnegative matrix factorizations. In: Gervasi O, Murgante B, Misra S, et al., eds. *International Conference on Computational Science and Its Applications.* Berlin, Germany: Springer; 2017:203-216.
- Del Buono N, Esposito F. On some practical issues related to Nonnegative Matrix Factorization in Microarray Data Analysis context. In Carletti M ed., *Series in Applied Sciences, Mathematical Modelling, Numerical and Data Analysis,* vol. 1. Mantua, Italy: Universitas Studiorum; 2018:109-130.
- Kim H, Park H. Sparse non-negative matrix factorizations via alternating non-negativity-constrained least squares for microarray data analysis. *Bioinformatics.* 2007;23:1495-1502. doi:10.1093/bioinformatics/btm134.
- Wang J, Vasaikar S, Shi Z, Greer M, Zhang B. WebGestalt 2017: a more comprehensive, powerful, flexible and interactive gene set enrichment analysis toolkit. *Nucleic Acids Res.* 2017;45:W130-W137. doi:10.1093/nar/gkx356.
- Maman S, Witz IP. A history of exploring cancer in context. *Nat Rev Cancer.* 2018;18:359-376. doi:10.1038/s41568-018-0006-7.
- Kalluri R. The biology and function of fibroblasts in cancer. *Nat Rev Cancer.* 2016;16:582-598. doi:10.1038/nrc.2016.73.
- Rinn JL, Bondre C, Gladstone HB, Brown PO, Chang HY. Anatomic demarcation by positional variation in fibroblast gene expression programs. *PLoS Genet.* 2006;2:e119. doi:10.1371/journal.pgen.0020119.
- Ozdemir BC, Pentcheva-Hoang T, Carstens JL, et al. Depletion of carcinoma-associated fibroblasts and fibrosis induces immunosuppression and accelerates pancreas cancer with reduced survival. *Cancer Cell.* 2015;28:831-833. doi:10.1016/j.ccell.2015.11.002.
- Ohlund D, Elyada E, Tuveson D. Fibroblast heterogeneity in the cancer wound. *J Exp Med.* 2014;211:1503-1523. doi:10.1084/jem.20140692.
- Gascard P, Tlsty TD. Carcinoma-associated fibroblasts: orchestrating the composition of malignancy. *Genes Dev.* 2016;30:1002-1019. doi:10.1101/gad.279737.116.
- Nurmik M, Ullmann P, Rodriguez F, et al. In search of definitions: cancer-associated fibroblasts and their markers. *Int J Cancer.* 2020;146:895-905. doi:10.1002/ijc.32193.
- Bray F, Ferlay J, Soerjomataram I, Siegel RL, Torre LA, Jemal A. Global cancer statistics 2018: GLOBOCAN estimates of incidence and mortality worldwide for 36 cancers in 185 countries. *CA Cancer J Clin.* 2018;68:394-424. doi:10.3322/caac.21492.
- Edgar R, Domrachev M, Lash AE. Gene expression omnibus: NCBI gene expression and hybridization array data repository. *Nucleic Acids Res.* 2002;30:207-210.
- Herrera M, Islam A, Herrera A, et al. Functional heterogeneity of cancer-associated fibroblasts from human colon tumors specific prognostic gene expression signature. *Clin Cancer Res.* 2013;19:5914-5926. doi:10.1158/1078-0432.CCR.
- Christensen J, El-Gebali S, Natoli M, et al. Defining new criteria for selection of cell-based intestinal models using publicly available databases. *BMC Genomics.* 2012;13:274. doi:10.1186/1471-2164-13-274.
- Marsh T, Wong I, Sceneay J, et al. Hematopoietic age at onset of triple-negative breast cancer dictates disease aggressiveness and progression. *Cancer Res.* 2016;76:2932-2943.
- Bauer M, Su G, Casper C, He R, Rehrauer W, Friedl A. Heterogeneity of gene expression in stromal fibroblasts of human breast carcinomas and normal breast. *Oncogene.* 2010;29:1732-1740. doi:10.1038/ncr.2009.463.
- Yeung TL, Leung CS, Wong KK, et al. TGF-beta modulates ovarian cancer invasion by upregulating CAF-derived versican in the tumor microenvironment. *Cancer Research.* 2013;73:5016-5028. doi:10.1158/0008-5472.CAN.
- Helleday T, Eshtad S, Nik-Zainal S. Mechanisms underlying mutational signatures in human cancers. *Nat Rev Genet.* 2014;15:585-598. doi:10.1038/nrg3729.
- Burns MB, Leonard B, Harris RS. Apobec3b: pathological consequences of an innate immune DNA mutator. *Biomed J.* 2015;38:102-110. doi:10.4103/2319-4170.148904.
- Ziegler SJ, Liu C, Landau M, et al. Insights into DNA substrate selection by apobec3g from structural, biochemical, and functional studies. *PLoS ONE.* 2018;13:e0195048. doi:10.1371/journal.pone.0195048.
- Jin J, Cardozo T, Lovering RC, Elledge SJ, Pagano M, Harper JW. Systematic analysis and nomenclature of mammalian f-box proteins. *Genes Dev.* 2004;18:2573-2580. doi:10.1101/gad.1255304.
- Fernandez-Saiz V, Targosz BS, Lemeer S, et al. SCFFbxo9 and CK2 direct the cellular response to growth factor withdrawal via Tel2/Tti1 degradation and promote survival in multiple myeloma. *Nat Cell Biol.* 2013;15:72-81. doi:10.1038/ncb2651.
- Houben AJ, Moolenaar WH. Autotaxin and LPA receptor signaling in cancer. *Cancer Metastasis Rev.* 2011;30:557-565. doi:10.1007/s10555-011-9319-7.
- Somech R, Lev A, Grisaru-Soen G, Shiran SI, Simon AJ, Grunebaum E. Purine nucleoside phosphorylase deficiency presenting as severe combined immune deficiency. *Immunol Res.* 2013;56:150-154. doi:10.1007/s12026-012-8380-9.
- Lochhead P, Wickman MG, Mezna Olson MF. Activating ROCK1 somatic mutations in human cancer. *Oncogene.* 2010;29:2591-2598.
- Whatcott CJ, Ng S, Barrett MT, Hostetter G, Von Hoff DD, Han H. Inhibition of ROCK1 kinase modulates both tumor cells and stromal fibroblasts in pancreatic cancer. *PLoS ONE.* 2017;12:e0183871. doi:10.1371/journal.pone.0183871.
- Gatza CE, Oh SY, Blobel GC. Roles for the type III TGF-beta receptor in human cancer. *Cell Signal.* 2010;22:1163-1174. doi:10.1016/j.cellsig.2010.01.016.
- Jenkins LM, Singh P, Varadaraj A, et al. Altering the proteoglycan state of transforming growth factor beta type III receptor (TβRIII)/betaglycan modulates

- canonical Wnt/ $\beta$ -catenin signaling. *J Biol Chem.* 2016;291:25716-25728. doi:10.1074/jbc.M116.748624.
52. Gatza CE, Holtzhausen A, Kirkbride KC, et al. Type III TGF- $\beta$  receptor enhances colon cancer cell migration and anchorage-independent growth. *Neoplasia.* 2011;13:758-770.
53. Tian X, Liu Z, Niu B, et al. E-cadherin/ $\beta$ -catenin complex and the epithelial barrier. *J Biomed Biotechnol.* 2011;2011:6. doi:10.1155/2011/567305.
54. Du W, Liu X, Fan G, et al. From cell membrane to the nucleus: an emerging role of e-cadherin in gene transcriptional regulation. *J Cell Mol Med.* 2014;18:1712-1719. doi:10.1111/jcmm.12340.
55. Bakiri L, Macho-Maschler S, Custic I, et al. Fra-1/AP-1 induces EMT in mammary epithelial cells by modulating Zeb1/2 and TGF- $\beta$  expression. *Cell Death Differ.* 2015;22:336-350. doi:10.1038/cdd.2014.157.
56. Meng J, Li W, Zhang M, et al. An update meta-analysis and systematic review of tap polymorphisms as potential biomarkers for judging cancer risk. *Pathol Res Pract.* 2018;214:1556-1563. doi:10.1016/j.prp.2018.07.018.
57. Girard M, Poupon V, Blondeau F, McPherson PS. The DnaJ-domain protein RME-8 functions in endosomal trafficking. *J Biol Chem.* 2005;280:40135-40143. doi:10.1016/j.jprp.2018.07.018.
58. Xu L, Blackburn EH. Human Rif1 protein binds aberrant telomeres and aligns along anaphase midzone microtubules. *J Cell Biol.* 2004;167:819-830.
59. Lex A, Gehlenborg N, Strobelt H, Vuilleumot R, Pfister H. Upset: visualization of intersecting sets. *IEEE Trans Vis Comput Graph.* 2014;20:1983-1992.
60. Antigny F, König S, Bernheim L, Frieden M. Inositol 1,4,5 trisphosphate receptor 1 is a key player of human myoblast differentiation. *Cell Calcium.* 2014;56:513-521. doi:10.1016/j.ceca.2014.10.014.
61. Berridge MJ. The inositol trisphosphate/calcium signaling pathway in health and disease. *Physiol Rev.* 2016;96:1261-1296. doi:10.1152/physrev.00006.2016.
62. Unger CM, Kramer N, Unterleuthner D, et al. Stromal-derived IGF2 promotes colon cancer progression via paracrine and autocrine mechanisms. *Oncogene.* 2017;36:5341-5355. doi:10.1038/ncr.2017.116.
63. Ruehl MG, Erben U, Schuppan DB, et al. The elongated first fibronectin type III domain of collagen XIV is an inducer of quiescence and differentiation in fibroblasts and preadipocytes. *J Biol Chem.* 2005;280:38537-38543. doi:10.1074/jbc.M502210200.
64. Maroulakou IG, Damon B. Expression and function of Ets transcription factors in mammalian development: a regulatory network. *Oncogene.* 2001;19:6432-6442.
65. Zajacova M, Kotrbova-Kozak A, Cerna M. Expression of HLA-DQA1 and HLA-DQB1 genes in B lymphocytes, monocytes and whole blood. *International Journal of Immunogenetics.* 2017;45:128-137. doi:10.1111/iji.12367.
66. Hatakeyama S. TRIM family proteins: roles in autophagy, immunity, and carcinogenesis. *Trends Biochem Sci.* 2017;42:297-311. doi:10.1016/j.tibs.2017.01.002.
67. Lim L, Pervaiz S. Annexin 1: the new face of an old molecule. *FASEB J.* 2007;21:968-975. doi:10.1096/fj.06-7464rev.
68. Wang C, Yuan X, Yang S. IFT80 is essential for chondrocyte differentiation by regulating Hedgehog and WNT signaling pathways. *Exp Cell Res.* 2013;319:623-632.
69. Filmus J. Glypicans in growth control and cancer. *Glycobiology.* 2001;11:19R-23R.
70. Liu X, Sun LB, Gursel D, et al. The non-canonical ubiquitin activating enzyme UBA6 suppresses epithelial-mesenchymal transition of mammary epithelial cells. *Oncotarget.* 2017;8:87480-87493. doi:10.18632/oncotarget.20900.
71. Cannavo E, Gerrits B, Marra G, Schlapbach R, Jiricny J. Characterization of the interactome of the human MutL homologues MLH1, PMS1, and PMS2. *J Biol Chem.* 2007;282:2976-2986.
72. Huang J, Sun X, Gong X, et al. Rearrangement and expression of the immunoglobulin mu-chain gene in human myeloid cells. *Cell Mol Immunol.* 2013;11:94-104. doi:10.1038/cmi.2013.45.
73. Shen FF, Pan Y, Li JZ, et al. High expression of HLA-DQA1 predicts poor outcome in patients with esophageal squamous cell carcinoma in northern china. *Medicine (Baltimore).* 2019;98:e14454. doi:10.1097/MD.00000000000014454.
74. Lasho T, Finke C, Zblewski D, et al. Novel recurrent mutations in ethanolamine kinase 1 (ETNK1) gene in systemic mastocytosis with eosinophilia and chronic myelomonocytic leukemia. *Blood Cancer J.* 2015;5:e275. doi:10.1038/bcj.2014.94.
75. Valdes-Rives S, Gonzalez-Arenas A. Autotaxin-lysophosphatidic acid: from inflammation to cancer development. *Mediators Inflamm.* 2017;2017:9173090-9173015. doi:10.1155/2017/9173090.
76. Tigyí J, Yue G, Norman D, et al. Regulation of tumor cell—microenvironment interaction by the autotaxin-lysophosphatidic acid receptor axis. *Adv Biol Regul.* 2019;71:183-193. doi:10.1016/j.jbior.2018.09.008.